The Spatial Organization of Lipid Synthesis in the Yeast *Saccharomyces cerevisiae* Derived from Large Scale Green Fluorescent Protein Tagging and High Resolution Microscopy*[S]

Klaus Natter‡, Peter Leitner‡, Alexander Faschinger‡, Heimo Wolinski‡, Stephen McCraith§¶, Stanley Fields§‖, and Sepp D. Kohlwein‡ ‡‡**

The localization pattern of proteins involved in lipid metabolism in the yeast *Saccharomyces cerevisiae* was determined using C-terminal green fluorescent protein tagging and high resolution confocal laser scanning microscopy. A list of 493 candidate proteins (~9% of the yeast proteome) was assembled based on proteins of known function in lipid metabolism, their interacting proteins, proteins defined by genetic interactions, and regulatory factors acting on selected genes or proteins. Overall 400 (81%) transformants yielded a positive green fluorescent protein signal, and of these, 248 (62% of the 400) displayed a localization pattern that was not cytosolic. Observations for many proteins with known localization patterns were consistent with published data derived from cell fractionation or large scale localization approaches. However, in many cases, high resolution microscopy provided additional information that indicated that proteins distributed to multiple subcellular locations. The majority of tagged enzymes localized to the endoplasmic reticulum (91), but others localized to mitochondria (27), peroxisomes (17), lipid droplets (23), and vesicles (53). We assembled enzyme localization patterns for phospholipid, sterol, and sphingolipid biosynthetic pathways and propose a model, based on enzyme localization, for concerted regulation of sterol and sphingolipid metabolism that involves shuttling of key enzymes between endoplasmic reticulum, lipid droplets, vesicles, and Golgi. ***Molecular & Cellular Proteomics 4:662–672, 2005.***

Biological membranes are characterized by a highly complex mixture of lipids that are key determinants of the biophysical parameters of membranes, such as fluidity, permeability, and signaling functions. Thus, lipids affect structure and function of peripheral and integral membrane proteins, and thus play a pivotal role in organelle (membrane) function. In the yeast *Saccharomyces cerevisiae*, the lipid composition appears rather simple, consisting mainly of glycerophospholipids, sphingolipids, and ergosterol (1); however, recent advances in analytical techniques such as nanoelectrospray ionization tandem mass spectrometry (2) have unveiled a great degree of heterogeneity within the molecular species of phospholipids. Furthermore subcellular membranes differ not only in their lipid composition in terms of lipid classes, they are also characterized by a distinct distribution of molecular species of phospholipids (3). Because only a few membranes harbor enzymes involved in lipid synthesis, this heterogeneity may be established by localized synthesis, localized degradation, and selective trafficking of membrane lipids. Interestingly apparently "linear" pathways for the synthesis of major membrane lipids involve multiple organelles: the synthesis of phosphatidylserine by a synthase (Cho1p) occurs in the endoplasmic reticulum (ER)[1] and is followed by decarboxylation to phosphatidylethanolamine in the mitochondrial inner membrane (by Psd1p) or Golgi/vacuoles (by Psd2p). Subsequently phosphatidylethanolamine is converted by three-step methylation (by Cho2p and Opi3p) to the major yeast membrane phospholipid, phosphatidylcholine, again in the ER. Cell fractionation experiments unveiled the existence of specific subfractions of the endoplasmic reticulum (plasma-membrane associated ER and mitochondria-associated ER) that were found to be highly enriched in lipid biosynthetic activities (4, 5). A potential function of these subfractions in interorganelle lipid trafficking was suggested; however, the mechanisms involved in establishing apparent asymmetries in lipid enzyme distribution within organelles are unknown. Furthermore the mechanisms that control a defined molecular species distribution in subcellular membranes are obscure (3, 6). On the other hand, specific regulatory mechanisms obviously do exist to adjust lipid composition to altered cellular conditions as

From the ‡Institute of Molecular Biosciences, Spezialforschungsbereich Biomembrane Research Center, University of Graz, Schubertstr. 1, A8010 Graz, Austria and the §Departments of Genome Sciences and Medicine and the ‖Howard Hughes Medical Institute, University of Washington, Seattle, Washington 98195

Received, September 8, 2004, and in revised form, February 11, 2005

Published, MCP Papers in Press, February 16, 2005, DOI 10.1074/mcp.M400123-MCP200

[1] The abbreviations used are: ER, endoplasmic reticulum; GFP, green fluorescent protein; eGFP, enhanced GFP; LD, lipid droplet; PTS, peroxisomal targeting sequence; NVJ, nuclear-vacuolar junction.

exemplified by the changes in phosphatidylserine molecular species distribution in the plasma membrane upon introduction of a subtle alteration in fatty acid chain elongation in the ER, mainly affecting sphingolipid synthesis (3).

To better understand the spatial organization of lipid synthesis, we tagged a large number of known and predicted proteins involved in lipid synthesis and membrane biogenesis with GFP and analyzed their subcellular localization by high resolution fluorescence microscopy. Enzymes of specific metabolic pathways are typically concentrated in one or a few subcellular structures, *e.g.* glycolytic enzymes in the cytosol or fatty acid β-oxidation in peroxisomes. Due to this compartmentalization of metabolic pathways, knowledge about the subcellular destination of an uncharacterized protein may be key to elucidate its function. In addition, assembling complete pathways in terms of spatial organization may help to better understand lipid trafficking pathways and regulatory features controlling membrane lipid composition and may also contribute to filling the white spots on the lipid pathway maps.

Protein localization at large scale follows two principal microscopic strategies, either based on immunofluorescence detection or GFP fusions. Kumar *et al.* (7) used a transposon-based approach to create epitope-tagged proteins that were subsequently detected by immunofluorescence microscopy. The tagging of proteins with GFP from *Aequorea victoria* or numerous color variants derived thereof is a well established and widely used technique for *in vivo* localization studies (8–11) despite a potential risk of artifacts inherent to all tagging approaches. GFP is a protein of ~29 kDa and may cause mislocalization of a tagged protein, *e.g.* by masking targeting sequences or by interfering with posttranslational modifications like N-terminal myristoylation or the C-terminal attachment of glycosylphosphatidylinositol anchors. Another common problem associated with chromosomally integrated GFP constructs is the low expression level of the fused gene under the control of its endogenous promoter (10, 11). This problem may be avoided by the use of episomal fusion constructs expressed under the control of heterologous regulatable or constitutive promoters. Although changes in protein abundance that are dependent on growth phase, growth conditions, or stage of the cell cycle are likely to be lost under these conditions, episomal plasmids are the method of choice for detecting low abundance proteins and for use in multiple recipient strains, allowing protein localization in various mutant backgrounds to be addressed.

In the present study, we attempted to generate high resolution localization data for a subset of the yeast proteome consisting of almost 500 yeast open reading frames that were selected based on their predicted role in lipid metabolism. To generate GFP-tagged proteins, we used recombination cloning that was previously used for constructing strains suitable for two-hybrid analysis and glutathione *S*-transferase fusions (12–15). Genes of interest were cloned into a centromeric plasmid containing the constitutive, moderately strong *TEF1* promoter, the *URA3* selection marker, and enhanced green fluorescent protein (eGFP). The localization data demonstrate the importance of high resolution microscopy for the classification of the suborganellar distribution of proteins and the characterization of proteins of unknown function. Image data together with experimental details are stored in a web-accessible data base, YPL.db, which can be searched and viewed at ypl.uni-graz.at (16, 17). Furthermore YPL.db can be accessed through *Saccharomyces* Genome Database (18).

MATERIALS AND METHODS

Strains and Plasmids—The diploid strain FY1679d, *ura3–52/ura3–52*; *trp1Δ63/TRP1*; *leu2Δ1/LEU2*; *his3Δ200/HIS3*, was used for all transformations. Plasmid p416TEF (*CEN*, *AmpR*, *URA3*) was obtained from Martin Funk (19). Plasmid pHGFP-S65T was obtained from Clontech. For construction of pKNeGFP, plasmid p416TEF was modified to contain the recombination domain from pOAD (13) and the eGFP coding region from pHGFP-S65T. Briefly eGFP was first amplified using the Expand high fidelity PCR system (Roche Diagnostics) and the following oligonucleotides: F1, 5′-AAGCAGGCTTCGAATTCCAGCTGACCACCATGGCAATTCCCGGGGATCCGATGAGTAAAGGAGAAGAACTTTT-3′; and R1, 5′-AACCACTTTGTACAAGAAAGCTGGGTTCTTGTACAGCTCGTCCATGCCG-3′. The product of this PCR was used as a substrate for a second round of PCR to add additional sequence homologous to p416TEF. The primers used for this reaction were F2, 5′-TCTAGAACTAGTGACAAGTTTGTACAAAAAAGCAGGCTTCGAATTCCAGCTGACCACCATG-3′; and F3, 5′-AACCCAGCTTTCTTGTACAAAGTGGTTTAACTCGAGTCATGTAATTAGTTATGTCACGCTTACATTCACGCCCTC-3′. DNA fragments were co-transformed with the linearized, XhoI-digested p416TEF plasmid using the lithium acetate method (20).

Construction of GFP Fusions—Yeast strains bearing episomal GFP constructs were generated according to the method of Ma *et al.* (14). PCR clones from Research Genetics (now Invitrogen), including start and stop codons and flanked by universal sequence extensions (CGAATTCCAGCTGACCACC at the 5′-end and CATGGCAATTCCCGGGGATC at the 3′-end), were modified and amplified in two PCRs. In a first step the stop codons were replaced by amino acid coding sequences. Codons TAA and TAG were replaced by TAT (Tyr) with primer GATCCCCGGGAATTGCCATG**ATA**, and the stop codon TGA was replaced by TGC (Cys) with primer GATCCCCGGGAATTGCCATG**GCA**. Bold nucleotides indicate changed codon sequences. The forward primer was CGAATTCCAGCTGACCACCATG in both cases. In a second PCR, regions homologous to plasmid p416TEF were added up- and downstream of the universal sequences. Primers used were 5′-ACTAGTGACAAGTTTGTACAAAAAAGCAGGCTTCGAATTCCAGCTGACCACCATG-3′ and 5′-GACCACTCCAGTGAAAAGTTCTTCTCCTTTACTCATCGGATCCCCGGGATTGCCATG-3′. After amplification using *Taq* DNA polymerase (Roche Diagnostics) DNA fragments were co-transformed with the linearized, EcoRI/SmaI-digested pKNeGFP plasmid using the lithium acetate method (20), and uracil prototrophic transformants were selected. On average, 20 transformants were obtained per ng of PCR product, and routinely, 12 colonies were selected for microscopic screening. GFP-positive clones were analyzed with respect to the size of the GFP fusion by Western blotting of total cell extracts, which were prepared by the method of Horvath and Riezman (21).

Microscopy—Cells were cultivated in microtiter plates overnight, concentrated by centrifugation, spotted onto microscopy slides coated with 0.5-mm-thick agar medium, and incubated at 30 °C for 4–8 h. Up to 32 colonies were spotted onto single slides and covered

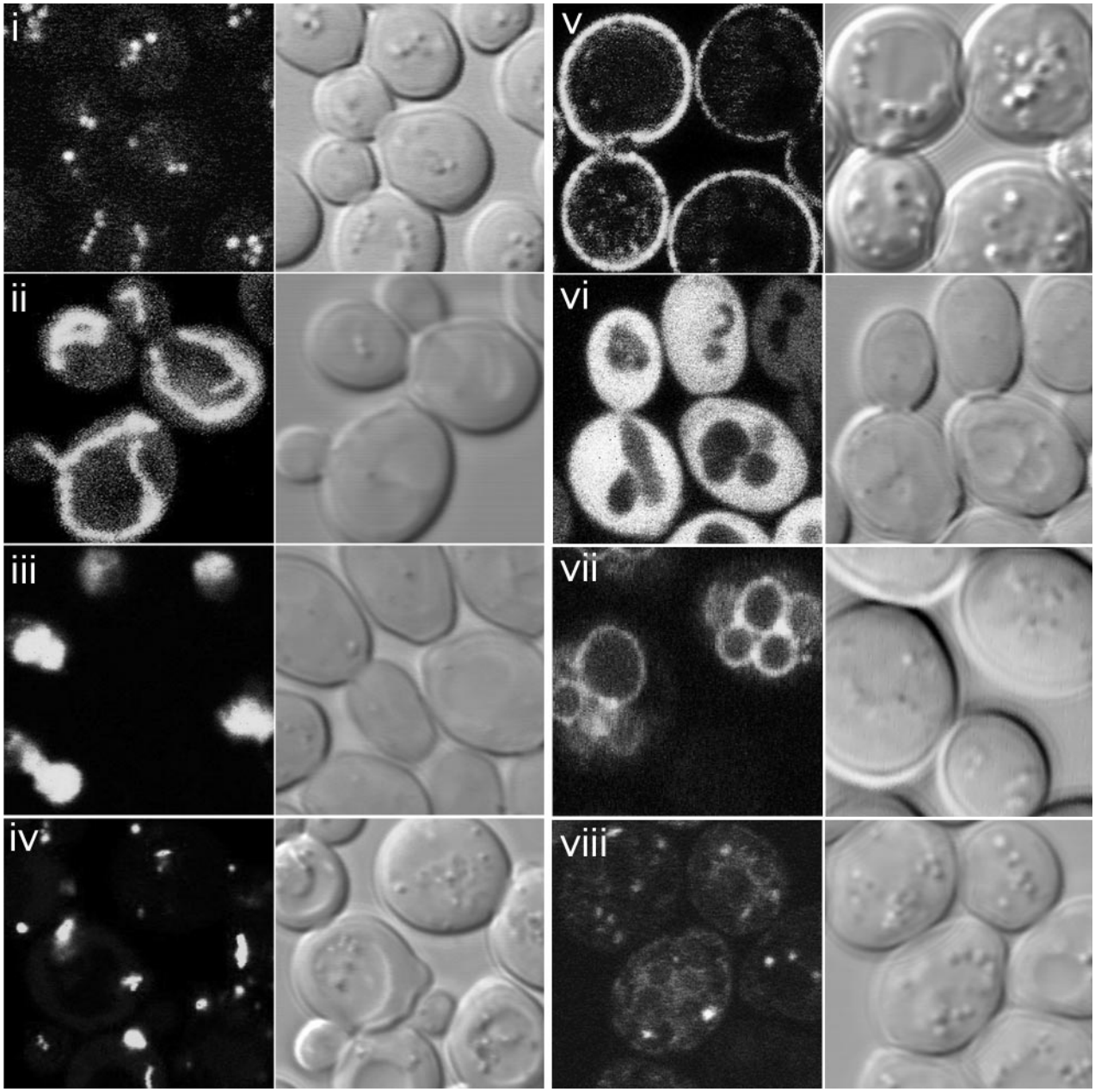

FIG. 1. **Reference localization patterns.** *i*, lipid droplets; *ii*, mitochondria; *iii*, nuclear lumen; *iv*, peroxisomes; *v*, plasma membrane; *vi*, cytosol; *vii*, vacuolar membrane; *viii*, Golgi + vacuolar membrane. (See Fig. 3 for ER reference localizations and Supplemental Fig. S1 for reference stainings with vital dyes.)

with a large coverslip prior to microscopy. Fluorescence microscopy was performed on a Leica TCS 4d confocal microscope with appropriate laser and filter settings for optimized GFP fluorescence and transmitted light (differential interference contrast) detection (9). Images were recorded in multiple optical sections and stored in an Oracle-based, web-accessible image data base, YPL.db (16, 17). Images were evaluated, and localizations were assigned independently by at least two researchers based on established reference localization patterns (Fig. 1). Vital stainings (9) and defined reference localization patterns (GFP-tagged marker proteins) were used to assign localizations to ambiguously scored data, *e.g.* different types of "punctate" structures (Supplemental Fig. S1).

RESULTS AND DISCUSSION

Selection of Target Proteins—We attempted tagging with GFP of 493 proteins, selected on their potential participation in lipid synthesis and membrane assembly in yeast, to identify their subcellular localization by high resolution fluorescence microscopy. The selection of relevant genes relied on the functional category "lipid, fatty acid, and sterol metabolism" of *Saccharomyces* Genome Database (18), Munich Information Center for Protein Sequences (22), and YPD™ data bases and interacting partners that were identified in two-

hybrid (23) and genetic screens for synthetic lethality as well as regulatory factors, lipid-binding and lipid-modified proteins, and proteins of unknown function with homologies to lipid metabolic enzymes. About 20% of these gene products were of unknown function; 40 proteins of this selection were of unknown subcellular localization according to their Gene Ontology annotations. A table listing the selected proteins together with gene ontology terms for biological process, molecular function, and cellular component as well as the protein annotations from the *Saccharomyces* Genome Database (18) are available on line as supplemental data (Supplemental Table S1).

GFP Tagging and Localization Approach—Large scale tagging with GFP was performed based on recombination cloning as described under "Materials and Methods," making use of PCR-amplified genomic DNA fragments of the individual genes (Invitrogen). These DNA fragments contain the entire reading frame, including start ATG and stop codons, and universal 20-mer extensions at the 5′- and 3′-ends common to all genes. To allow C-terminal GFP fusion by recombination cloning, stop codons were removed, and flanking sequences homologous to the recipient vector were added by PCR. This procedure introduced a linker sequence of nine amino acids between the C-terminal amino acid of the tagged protein and GFP. Cotransformation of the linearized recipient vector with the PCR fragments into strain FY1679 yielded transformants for 467 of the selected genes. 400 of these transformants (81%) displayed a GFP signal, demonstrating recircularization of the plasmid. Clones that did not yield GFP fusions typically represented large genes (>3000 bp), suggesting that the PCR steps for amplification, stop codon removal, and addition of homologous sequences may have introduced errors in long sequences that prevented successful recombination or translation.

Of the 400 clones that displayed GFP fluorescence, ~62% (248 protein fusions) localized to subcellular structures other than cytoplasm or allowed identification of organellar structures in addition to a cytosolic signal. Compared with previous large scale localization approaches by Huh *et al.* (10) and Kumar *et al.* (7), 52% (209 clones) of our data are compatible with at least one of these studies. For 87 constructs (22%) we obtained divergent results; however, there was very little agreement about localization of these proteins between the previous large scale studies, suggesting interference of any type of tagging with proper localization of these proteins. High resolution microscopic analysis provided additional information for 61 (15%) GFP fusions (*i.e.* dual localization patterns not detectable by epifluorescence microscopy), and localizations for 43 proteins (10%) were determined for the first time in a large scale approach. The complete data set is available on line as supplemental data (Supplemental Table S1) and compiles data from previous large scale approaches (7, 10) and also includes Gene Ontology terms and annotations from the *Saccharomyces* Genome Database (18).

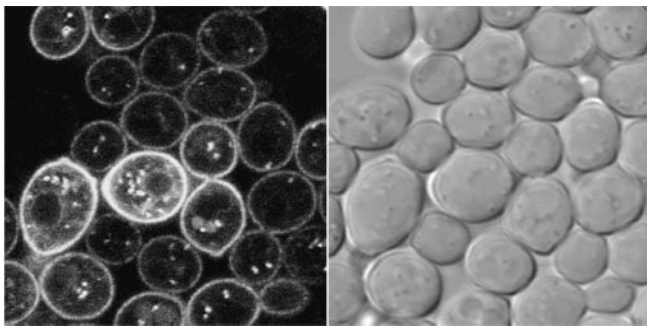

FIG. 2. **Robust subcellular localization of the plasma membrane protein Git1p, independent of expression level.** The image shows a strong gradient of expression levels in the cell population due to expression from an episomal plasmid. Evaluation of large numbers of cells aided in localization assignment, independent of expression level of the tagged protein.

Overexpression of GFP Fusions Results in Stable Localization Patterns—Potential mislocalization of fusions is clearly a limitation to the GFP tagging approach. A considerable fraction of these proteins belongs to a class of sequences subject to misfolding or steric hindrance due to the GFP tag. A second class comprises proteins bearing a targeting signal at their C terminus like farnesylation, glycosylphosphatidylinositol anchor attachment, and the peroxisomal targeting sequence PTS1. Surprisingly most of the peroxisomal proteins bearing PTS1 localized correctly, reflecting the fact that PTS1 is not the only targeting signal in these proteins.

The endoplasmic reticulum plays a predominant role not only in lipid metabolism (see below) but also in processing of proteins destined for delivery to other parts of the cell via the secretory pathway. Therefore, observation of GFP-tagged proteins in the ER has to be critically evaluated in view of a potential retention of secretory proteins due to overexpression and/or the tag. Of 92 ER-resident proteins analyzed in this study only nine showed divergent localizations compared with focused, non-large scale studies, *i.e.* Tip1p, Rvs167p, Fen2p, Vrg4p, Aur1p, Fps1p, Pik1p, Ncr1p, and Plb1p. For Tip1p and Plb1p, mislocalization was not unexpected due to interference with C-terminal glycosylphosphatidylinositol anchoring (24). On the other hand, further analysis of the retention mechanisms of the other proteins to the ER might provide clues as to the delivery machinery and signals required for their proper targeting.

We found that most of the enzymes investigated in this study localized with a robust signal that was independent of the expression level of the of plasmid-borne fusion constructs that varied considerably within a given cell population. This "gradient" of expression underscores the great potential of yeast for localization studies, providing excellent statistics and great confidence in a localization pattern among a cell population (Fig. 2). In general, functional complementation of a mutant phenotype by a GFP fusion is considered a crucial determinant of proper localization. However, there is generally

no proof that the fluorescence pattern observed corresponds to a complementing activity; for example, only 5% of a fusion protein may be functional and properly localized, whereas 95% may be mislocalized and observed in the microscope.

Additionally expression observed using an endogenous promoter, although crucial for determining cell cycle- and growth phase-specific expression and localization, may not reflect the wild-type expression due to potential up-regulation of a GFP fusion that is not fully functional.[2] Furthermore expression under an endogenous promoter may be too low to allow microscopic detection of many fusions (~60% of the yeast proteome displays a Codon Adaptation Index of 0.15 or below, indicating a low level of expression, which is particularly true for genes encoding lipid enzymes). Nevertheless GFP tagging provides immense advantages due to the ease of constructing and detecting protein fusions in living cells, avoiding the artifacts, technical limitations, and labor costs associated with immunolocalization and cell fractionation studies. In addition, tagging by recombination cloning is a versatile tool to generate a large number of GFP fusions for localization studies in various mutant backgrounds, aiding investigations on protein localization in the context of lipid malfunction. Because in mammalian cells tagging of episomal constructs is the only feasible approach in similar types of large scale localization studies (25), statistics obtained from the yeast studies provide great confidence that localization typically is very robust and over a wide range independent of expression levels.

The Need for High Resolution Imaging—High resolution live cell microscopy of cells expressing GFP fusions not only allows assignment of proteins to organelles but also to suborganellar structures. In addition, the characterization of the dynamic properties of organelles and of processes like the distribution of proteins along the secretory pathway also contributes to the functional classification of proteins. The requirement for a concise description of localization patterns and dynamic protein distribution exceeds the possibilities of a strictly structured annotation system such as provided by the Gene Ontology consortium (26). Efforts toward a standardized description for quantitative image data are under way (Open Microscopy Environment (27)). Until the advent of computerized description tools to "quantitate" image and localization data, we suggest that the depiction of original images, in addition to an interpretation of the localization pattern, should be included in the localization annotation. We have thus created a data base of high resolution confocal images of yeast proteins tagged with GFP with individual comments on localization information. This data base is accessible at ypl.unigraz.at. The collection of images contains not only data derived from this study but additional results from numerous specialized localization experiments. The data base development is an ongoing project and open to submission of high resolution live cell images from the yeast community. Image submission is achieved via an on-line web form (16, 17).

The Yeast Lipid Proteome: the Central Role of the Endoplasmic Reticulum—Table I summarizes the localization data obtained in this study. The large number of ER-localized proteins confirms previous analyses derived mainly from cell fractionation experiments that the ER is the major site of lipid synthesis, *e.g.* synthesis of sphingolipids, sterols, and phospholipids. Together with lipid droplets and peroxisomes, two compartments also known to be involved in lipid turnover, more than half of the non-cytosolic proteins were observed to localize at typical lipid metabolism organelles. Fifteen percent of the constructs localized to the nucleus, reflecting the transcription factors that were included in our study.

Sterols and Sphingolipids: Metabolic Flux between Cytosol, ER, Vesicles, and Lipid Droplets—The localization patterns of enzymes involved in sphingolipid and sterol metabolism are illustrated in Fig. 3. Early steps of sterol synthesis (Fig. 3*A*) up to squalene are cytosolic except for the committed step of sterol synthesis catalyzed by the ER-bound enzymes Hmg1p and Hmg2p. The association of these early steps of sterol synthesis with the membrane clearly implies a regulatory role of the enzymes in sensing membrane sterol content (28). Later steps are predominantly localized to the endoplasmic reticulum. Two principal deviations were observed from the typical ER association in the post-squalene pathway; several enzymes, including squalene epoxidase (Erg1p), squalene synthase (Erg7p), 3-keto sterol reductase (Erg27p), and sterol Δ^{24}-methyltransferase (Erg6p), were present in the ER but also associated with lipid droplets, consistent with previous studies (29–32). Such a dual localization pattern can be observed with most proteins associated with LDs that are also present in the ER (29–31, 33). The LD core consists largely of triglycerides and sterol intermediates esterified to fatty acids (34). Major sterol intermediates found in LDs are lanosterol, zymosterol, and fecosterol, which are the products of the Erg7, Erg27, and Erg6 proteins, respectively. Interestingly these enzymes not only localized to the ER, as did the majority of sterol-synthesizing enzymes, but also to LDs. This dual localization may thus reflect a specific regulatory mechanism of sterol biosynthesis that sequesters these enzymes together with their products in the LD storage compartment. Thus, excess synthesis of steryl esters may limit the availability of these enzymes in the ER, providing a rapid mechanism for controlling flux through the sterol biosynthetic pathway.

A second deviation from the typical ER pattern is represented by the proteins Erg2p and Erg25p, which are distributed between ER and vesicles. This observation will be discussed below.

Whereas all proteins in the ergosterol biosynthetic pathway yielded positive signals in this study, several enzymes involved in ceramide biosynthesis (Fig. 3*B*) proved to be very sensitive to tagging with GFP. Synthesis of essential very-long-chain fatty acids (C_{26} carbon atoms) is catalyzed by the

[2] S. D. Kohlwein, unpublished observations.

TABLE I
Subcellular distribution of the lipid proteome

Proteins localized to more than one compartment are listed in each relevant compartment and are marked with an asterisk.

Endoplasmic reticulum (92)[a]	ALG9, AQY1, ARE1, ARE2, AUR1, AYR1*, BOS1*, CHO1, CHO2, COX10*, CSG2*, CSR1*, CYB5, DGA1*, DPL1, DPP1*, EHT1*, ELO1, EPT1*, ERG1*, ERG2*, ERG24*, ERG25*, ERG26, ERG27*, ERG3*, ERG4, ERG5, ERG6*, ERG7*, ERG9*, EUG1*, FAA1*, FAA4*, FAT1*, FEN1, FEN2, FPS1, GAA1*, GOG5, GPI11, GPI2, GPI8, GSF2, GUP1, HMG1*, INP54*, IRE1, LCB2, LPP1*, MEC1, NCP1, NCR1, OLE1, OPI3*, PAU7*, PHO86, PIK1*, PIS1*, PLB1*, PLB2*, PTC2*, RVS161*, SAC1*, SCS7*, SEC14*, SEC22*, SLA1*, SLC1*, SPC1, STE14, SUR2, SUR4, TIP1, TSC10*, YBR204C*, YDC1*, YDL015C*, YDL193W*, YDR018C*, YIL011W, YIM1*, YJU3*, YKL174C*, YKR003W*, YLR343W, YOL132W*, YOR059C*, LCB1, YJU3*, NVJ1, YDL015C*
Lipid droplets (23)	AYR1*, DGA1*, EHT1*, ERG1*, ERG27*, ERG6*, ERG7*, FAA4*, FAT1*, PDR16*, SLC1*, TGL1, TGL3, YBR042C, YBR204C*, YDL193W*, YDR018C*, YIM1*, YJU3*, YKR046C, YKR089C, YOR059C*, YOR081C
Peroxisomes (17)	ACS1, DCI1*, FAA2*, MDH3*, PEX10, PEX11, PEX13, PEX14, PEX17*, PEX19*, PEX2*, PEX3, PEX4, PEX5*, POT1, POX1, SPS19*
Plasma membrane (14)	ALR1*, ERG13*, FAA1*, FAA3, GIT1*, PDR16*, PDR17*, SNQ2, TSC10*, VHT1*, YJL145W*, YLL012W, YMR210W*, YOR009W*
Mitochondria (27)	AAD10, ACP1, AGP2, BIO2, CEM1*, COQ1, COX10*, COX4, CPT1, CRC1, CYB2, ECM1, ERG13*, GUT1, HEM1, PGS1, PPT2*, PSD1, RAM1*, RVS167, SCS3, TES1, TGL2, YAP1, YBR159W*, YDR531W, YPR140W
Vacuole, membrane (7)	ALR1*, AST2*, DPP1*, PIB1, PIB2, VPH1, YBR161W*
Vacuole, lumen (5)	GIT1*, PKA3*, SUR1*, YIL005W, YOR009W*
Nucleus, lumen (56)	ACS2, ADA2*, ALD2, ARD1*, BDF1, BET2*, BET4, CDC43*, DCI1*, ERG10, ERG13*, FMS1*, GCN5, GDS1, HAP2, HAP5, HDA1, HHF1, HHT1, HHT2, HTA3*, IML3*, INO4*, MRS6*, MUQ1*, NAT1, NDD1*, PGD1*, PIP2*, PKA3*, QRI2, RAD61, RAM2*, REX3, RFA2*, RFA3*, ROX1, RPD3*, RTT105, SCM3, SEC21, SKN7, SPO12, THI3, TOR2*, TUP1*, YCR072C*, YGL144C*, YGR198W*, YHR046C*, YJR107W*, YKL091C, YLR323C, YMR192W, YNL086W*, YOL054W
Nucleus, nucleolus (5)	ADA2*, HTA3*, IML3*, RER2*, YCR072C*
Nucleus, envelope (6)	ADR1, NDD1*, NUP53, OPI1, PCT1, YPC1*
Vesicles (55)	APG7*, APL2*, AQY2, AST2*, BET1, BOS1*, CDC48*, CSG2*, DPP1*, ERG2*, ERG20, ERG24*, ERG25*, ERG3*, ERG9*, EUG1*, FAA1*, GAA1*, GIT1*, GTS1, HES1*, HFA1*, HMG1*, INP54*, KES1*, LPP1*, OPI3*, PAU7*, PDR5*, PIS1*, PKA3*, PLB1*, PLB2*, PLB3*, PPT2*, PTC2*, RER2*, SCS7*, SEC22*, SUR1*, TSC10*, VHT1*, VPS4*, YBR108W*, YBR161W*, YDC1*, YDL015C*, YGR198W*, YJL072C, YKL174C*, YKR003W*, YKT6, YOL132W*, YOR009W*, YPC1*
Golgi (7)	BET3*, EPT1*, GDA1, PIK1*, PIS1*, SAC1*, SEC14*
Cytoskeleton (7)	SAC6*, SLA1*, SRV2*, YGR136W, YSC84*, YDR532C*, ZTA1*
Others (8)	SEC2*, VPS24, CEM1*, GCD7, HNM1, STT4, TOR1, YDR541C*
Cytoplasm (177)	AAD6, AAH1, ACB1, ACF2, ACH1, ALD6, APG1, APG12, APG13, APG16, APG7*, APG9, APL2*, ARD1*, AST1, AST2*, AUT7, BET2*, BET3*, BIO4, BMH1, BMH2, BOI2, BPL1, BTS1, CAR2, CDC43*, CDC48*, CSR1*, DAK1, DCI1*, DEP1, DJP1, DOA1, ECI1, EKI1, ERG8, FAA2*, FAB1, FAS2, FAT2, FMS1*, FPR1, FRQ1, GCR1, HAP3, HCS1, HES1*, HFA1*, HPR1, IDI1, IDP3, INO1, INO4*, INP51, IPT1, ISC1, JNM1, KES1*, LAS17, LCB4, LCB5, MAD2, MDH3*, MRS6*, MSS4, MUQ1*, MVD1, MYO2, NMT1, OYE2, OYE3, PDI1, PDR17*, PDR5*, PDX3, PEX17*, PEX19*, PEX2*, PEX5*, PGD1*, PHO84, PIP2*, PKC1, PLB3*, PLC1, PRM1, PRT1, PSD2, PTP1, RAM1*, RAM2*, RER2*, RFA2*, RFA3*, RIO2, RPD3*, RSP5, RTT101, RVS161*, SAC6*, SAH1, SEC14*, SEC2*, SEC24, SEC3, SEC59, SEC9, SFB2, SHE2, SHM2, SIN3, SIP1, SNF1, SOD1, SPS19*, SRV2*, STD1, SVL3, SWI6, TAH18, TDH1, TDH2, TDH3, TEL1, TOR2*, TPK1, TSC11, TSC3, TUB1, TUP1*, UBC5, UME6, UPC2, VMA2, VPS21, VPS30, VPS4*, YBR108W*, YBR159W*, YDL109C, YDR287W, YDR444W, YDR532C*, YDR541C*, YER024W, YFR016C, YGL039W, YGL144C*, YGR198W*, YHR001W, YHR046C*, YIR035C, YIR036C, YJL068C, YJL145W*, YJR083C, YJR107W*, YKL121W, YLR020C, YLR022C, YLR072W, YML131W, YMR210W*, YMR226C, YNL040W, YNL045W, YNL086W*, YNL094W, YNL134C, YPK1, YPL088W, YPR127W, YPT1, YSC84*, YSR3, ZTA1*

[a] The numbers in parentheses represent the number of proteins localized to that compartment.

proteins Elo2p, Elo3p, Ybr059wp, and Tsc13p, exclusively present in the ER and completely absent from vesicles. These proteins not only co-localize but act in a complex (35). In addition, Tsc13p was specifically enriched in nucleus-vacuole junctions of the endoplasmic reticulum membrane (36, 37), confirming that expression of the GFP fusion from the episomal plasmid is a reliable method to depict suborganellar distribution of proteins. The sphingosine (long-chain base) backbone of sphingolipids is synthesized in the ER as well, but the key enzyme Lcb1p also appeared to induce karmellae, which are stacks of ER membrane that are induced by specific membrane domains of Hmg1p and Hmg2p (38). The membrane structure of Lcb1p-induced karmellae, however, needs to be resolved at the electron microscopic level. The C-terminal GFP fusion of the serine palmitoyltransferase-associated protein Tsc3p, the hydroxylase Sur2p, and the inositol phosphotransferase Ipt1p showed cytosolic localizations. All these proteins are described as ER-localized enzymes (7, 39, 40). The reason for a higher proportion of mislocalized sphingolipid enzymes was not due to the expression from an episomal plasmid but may rather reflect particular sensitivity of these enzymes to C-terminal modification and/or interference

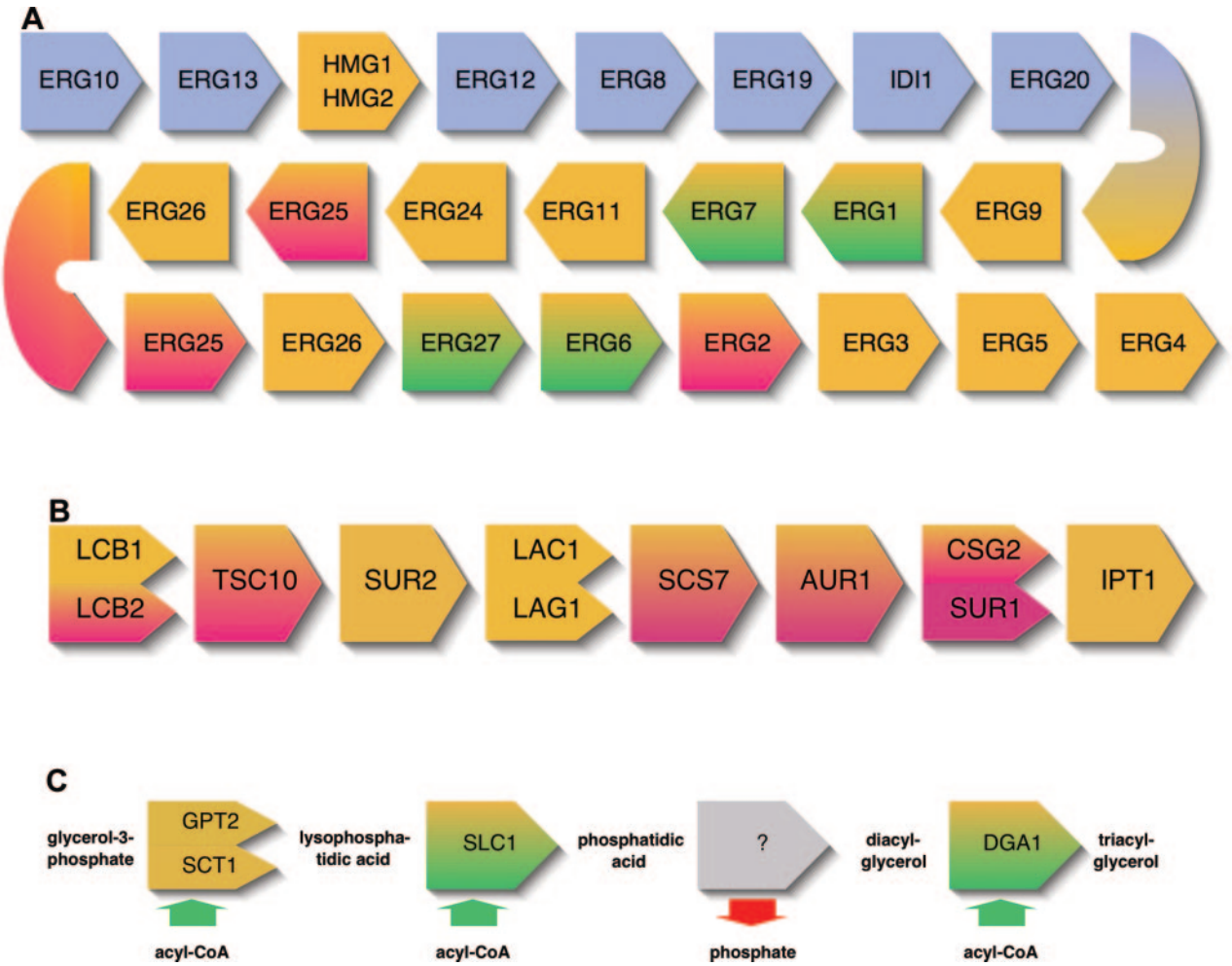

FIG. 3. **Localization of proteins involved in lipid metabolism: schematic representation of lipid biosynthetic pathways.** *A*, ergosterol biosynthesis. All enzymes of the pre-squalene pathway, except Hmg1p and Hmg2p, are cytosolic. Strongly hydrophobic squalene and the subsequent sterols are synthesized in the ER. Some of the enzymes of the post-squalene pathway show dual localization patterns to ER plus vesicles or ER plus lipid droplets. *B*, ceramide biosynthesis is accomplished almost exclusively by ER-bound enzymes; however, many of them show a dual localization to ER and vesicular structures. Vesicle number ranges from a few (Csg2p) up to 20 per cell (Sur1p), suggesting participation of several different vesicle types, *e.g.* COP vesicles and Golgi. *C*, triacylglycerol biosynthesis. Localization patterns of "incomplete" pathways facilitate the identification of unknown proteins. The missing phosphatase activity converting phosphatidic acid to diacylglycerol, respectively, is predicted to be a lipid droplet protein. LD proteins of unknown function are, therefore, candidates for this activity. Color codes are: *blue*, cytosolic; *orange*, endoplasmic reticulum; *green*, lipid droplets; *red*, vesicles.

with complex formation. The putative ceramide synthases Lac1p and Lag1p (41) were not tagged in this work but are also described as ER proteins (42). Enzymes involved in ceramide synthesis and further processing (hydroxylation, mannosylation, and inositol phosphate attachment) are present in the ER membrane and vesicles, indicative of translocation into COP vesicles and Golgi. Interestingly the relative distribution between ER and vesicles changes quite considerably between the various enzymes in the pathway. Scs7p, a hydroxylase introducing a major structural alteration to the ceramide backbone, and the mannosyl transferase Sur1p stand out in this cascade as they localized predominantly to vesicles, rather than to the ER, and may thus play a major regulatory role in the pathway. A second set of ER proteins that is involved in sterol synthesis, including ergosterol biosynthetic enzymes Erg2p and Erg25p, also associated with small vesicles, providing a further hint as to the tight interaction between sterol and sphingolipid biosynthesis (43).

Identification of Protein Function by Localization—Identification of the localization of a protein may contribute significantly to its functional annotation as specific pathways are confined to different organelles. For instance, association with peroxisomes presumably restricts the function either to peroxisome biogenesis and degradation or peroxisome-related metabolism. Similar arguments hold for association with other organelles, providing rather straightforward avenues for functional tests. Localization maps also help to fill gaps of incomplete pathways as demonstrated for triglyceride synthesis

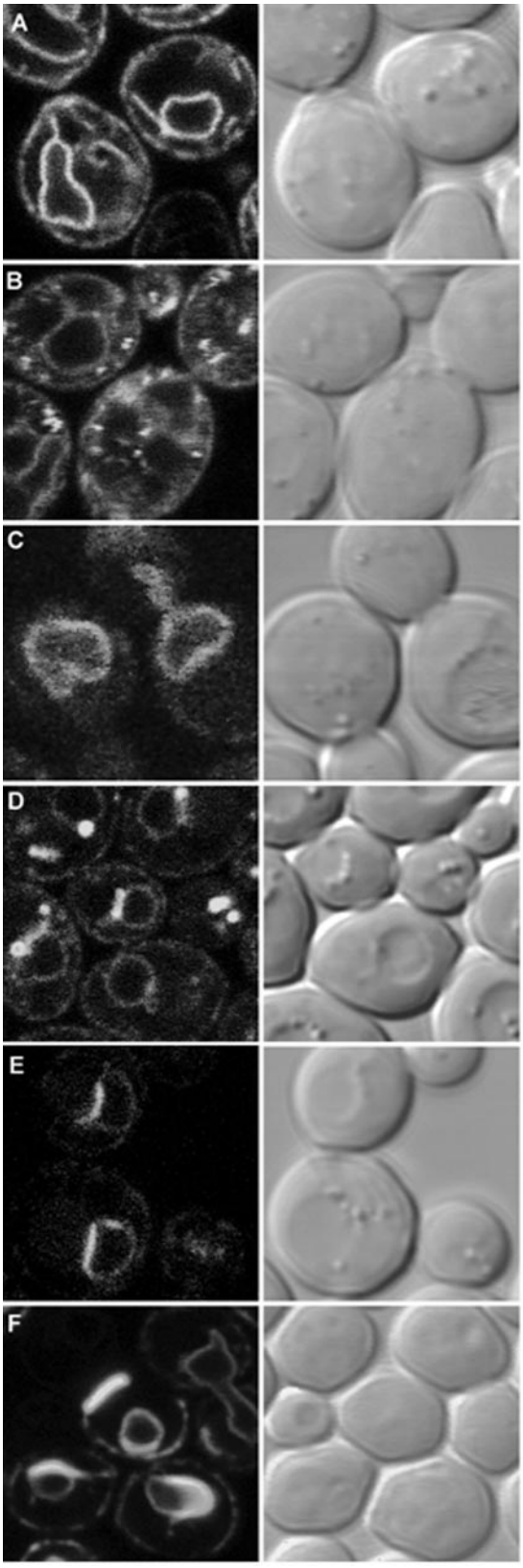

FIG. 4. **Characterization of ER subtypes.** The endoplasmic reticulum is a complex membrane system, appearing in many different shapes. The main types are peripheral and nuclear ER ("type I"), *e.g.* Cho1p (phosphatidylserine synthase) (*A*); rather diffuse peripheral and nuclear ER pattern, plus vesicles ("type II"), *e.g.* Sec22p (v-SNARE) (*B*); proteins localizing solely to the nuclear envelope ("type III"), *e.g.* Adr1p (transcription factor) (*C*); ER and lipid droplets ("type IV"), *e.g.* Faa4p (acyl-CoA synthetase; fatty acid activation) (*D*); nuclear-vacuolar junctions, *e.g.* Nvj1p (ER site of the junction; in contrast to the site on the vacuolar membrane) (*E*); karmellae, membrane proliferations due to overexpression of some proteins, *e.g.* Lcb1p (*F*).

(Fig. 3*C*); glycerol-3-phosphate acyltransferases Sct1p and Gpt2p were unambiguously characterized as localized to the ER. On the other hand, the acylglyceride fatty acyltransferase Slc1p and the diacylglycerol acyltransferase Dga1p both associated with the ER and lipid droplets. Thus, we predict that the not yet identified phosphatase activity required for dephosphorylation of phosphatidic acid to diacylglycerol is associated with LDs as well. Focusing molecular *in vivo* and *in vitro* analyses to hitherto uncharacterized LD proteins thus may greatly facilitate the identification of the relevant enzyme(s).

Suborganellar Organization of Lipid Biosynthetic Pathways—Confocal laser scanning microscopy resolves structures as small as 150 nm, providing insight into cellular organization on a suborganellar level. ER association of proteins involved in lipid synthesis appears in many different distributions, which might be relevant for enzyme function. A number of proteins, for instance, displayed a distinct and sharp association with the nuclear envelope, one or two membrane extensions from the nuclear envelope, and a network-like structure at the periphery of the cell in close vicinity to the plasma membrane (termed ER localization type I). The membrane extensions from the nuclear envelope may represent double bilayer membrane sheets that are also often in close proximity to the vacuolar surface (Fig. 4*A*). There is clearly a difference in the relative distribution of proteins between the nuclear and peripheral ER, ranging from almost exclusive nuclear ER to the other extreme of predominantly cortical localization, depending on the nature of the protein and on the growth conditions. Although these two compartments are presumably interconnected, the mechanisms promoting and keeping this asymmetry in protein and perhaps lipid distribution are unknown.

In contrast to the distinct type I ER localization, some of the characterized proteins displayed a more diffuse localization pattern to the nuclear envelope as well as to the cell periphery (type II; Fig. 4*B*). The extensions of the nuclear envelope are much less pronounced. However, in addition, a highly punctate pattern is observed that we interpret as COP vesicles involved in ER to Golgi and vice versa membrane and cargo cycling and Golgi. Thus, the associated lipid-synthesizing enzymes may cycle between the ER and the Golgi along the early steps of the secretory pathway. Computational analysis of the respective type I and type II ER protein sequences did not reveal any obvious structural differences, such as the

presence or absence of a certain number of transmembrane domains or ER retrieval sequences, suggesting that additional sequences and signals may be required for strict ER retention and/or recycling. Because all of the investigated proteins are membrane-associated or even integrated into the bilayer, the sorting signal may be related to the immediate lipid environment. Lipid-metabolizing enzymes face the problem that, by their activity, they continuously change the properties of their environment. Sterols, and sphingolipids harboring extended (up to C_{26}) carbon chains, tend to form specific lipid domains, termed rafts (44). Although raft formation is considered to be a process taking place at the Golgi, sterol and part of the sphingolipid components are synthesized in the ER, suggesting that raft preassembly may already take place at their site of synthesis, presumably together with the enzymes involved in their lipid processing.

A third class of proteins (type III; Fig. 4*C*) was identified that localizes exclusively to the nuclear envelope, including the transcription factor Adr1p and Pct1p, a structural and potentially regulatory enzyme involved in phosphatidylcholine synthesis. The appearance of Adr1p at the nuclear envelope is surprising given its function as a transcription factor with DNA binding activity (45), and overexpression was expected to result in cytosolic accumulation. Further studies will be required to address the relevance of the observed localization of Adr1p to the nuclear envelope.

Type IV ER proteins (Fig. 4*D*) localized to both the ER and lipid droplets. Our screening revealed two novel ER/LD proteins, encoded by the genes *YDR018c* and *YBR042c*; both proteins contain motifs common to the family of acyltransferases, supporting the assumption that LD proteins are very likely to be involved in lipid metabolism. LDs presumably derive from the ER (46); however, because specific targeting signals are not apparent, the mechanisms directing proteins to LDs and sequestering them in specific domains of the ER are unknown. Interestingly, in the absence of the neutral lipid core, LD-resident proteins remain in the ER (47).[3] Previous experiments have shown that Erg1p (squalene epoxidase) is not active on LDs due to the absence of the reductase required for its activity (30). Thus, localization to specific sites clearly does not predict an active function at this site but may reflect a regulatory function for a particular distribution to serve as a reservoir of enzyme for rapid mobilization and activation.

In addition to these four, rather frequent types of ER patterns, a number of proteins displayed particular localization patterns, like the nuclear-vacuolar junction, NVJ (36, 37), an ER domain of unknown function involved in microautophagy of nuclear components (48), or karmellae (38). NVJs (Fig. 4*E*) represent a specific subdomain of the ER established by the interaction of Nvj1p (nuclear envelope) and Vac8p (vacuolar membrane) proteins. However, whereas under wild-type levels of expression this asymmetric distribution occurs preferentially in stationary phase, it also became apparent upon overexpression of the Tsc13 and Nvj1 proteins during logarithmic growth. No other ER-resident protein investigated in this study accumulated in NVJs, consistent with a very specific pathway that directs proteins to this domain. The selective presence of Tsc13p (enoyl-CoA reductase) involved in fatty acid elongation in NVJs stands in marked contrast to other components of this pathway (Elo2p, Elo3p, and Ybr159wp), raising the intriguing possibility of localized fatty acid elongation (and further processing to sphingolipids) and/or regulation of the flux through the pathway by sequestering Tsc13p into a specific ER subdomain. Along this line, karmellae formation (Fig. 4*F*), which was previously discovered in the context of 3-hydroxy-3-methylglutaryl-CoA reductase overexpression (38), was observed with only one additional structurally and functionally unrelated protein involved in sphingolipid synthesis, Lcb1p (serine palmitoyltransferase catalytic subunit), suggesting a highly specific process restricted to a very limited number of proteins.

Interorganellar Distribution as a Regulatory Strategy—Synthesis of sterols and sphingolipids takes place predominantly in the endoplasmic reticulum membrane. However, some key steps, *e.g.* Erg2p (C-8 sterol isomerase) and Erg25p (C-4 sterol methyloxidase), were found to be also localized to vesicular structures and only to a minor part with the ER membrane. Erg25p was reported to be in a complex with Erg26p/Erg27p and interacts with an ER-resident "scaffolding" protein Erg28p (49), suggesting that the vesicle-associated Erg25p may represent an inactive "pool" of enzyme. Similarly components of the sphingolipid biosynthetic pathway localized to both ER and vesicles. This distribution between ER and vesicles may reflect a dynamic relocalization of the enzymes, coordinating sterol synthesis and sphingolipid processing, and membrane flow through the secretory pathway. Also relocalization of enzymatically inactive Erg1 protein from lipid droplets to the ER may be governed by changes in ER sterol content or upon specific cellular requirements for sterol synthesis. This principle of lipid-regulated localization of proteins and their activity is well established, for instance, in the process of sterol synthesis regulation in mammalian cells through sterol-regulatory element-binding protein localization and processing (for a review, see Ref. 50). Sterol-regulatory element-binding protein is a membrane-resident transcription factor that, dependent on ER cholesterol content, relocalizes to the Golgi where it encounters a specific protease, SCAP, which may cleave off the soluble part of sterol-regulatory element-binding protein, thus activating the transcription factor (50). Fatty acid desaturation in yeast follows a similar principle in that the Spt23 or Mga2 ER-resident membrane proteins become activated by a Cdc48p/Npl4p/Ufd1p- and unsaturated fatty acid-controlled proteasomal cleavage at the ER (51–53). The released fragments are subsequently able to turn on expression of genes harboring oleate-responsive ele-

[3] K. Natter and S. D. Kohlwein, unpublished results.

ments in their promoters, including *OLE1* (51, 53). We have previously observed that a conditional variant of the Ole1 protein, $Mdm2^{ts}$ (54), is reversibly sequestered within minutes into ER domains under restrictive conditions when the enzyme is unable to desaturate fatty acids. This relocalization process is suppressed by unsaturated fatty acid supplementation (55), clearly demonstrating that localization of this lipid-metabolizing enzyme is strongly dependent on its lipid environment, which may become modified by its own enzymatic activity. Such a model would also explain how changes in the lipid profiles by altered growth conditions or mutations result in major rearrangements of membrane lipid compositions. Thus, at least some of the key ER-resident lipid enzymes may also fulfill a major function as membrane sensors by means of relocating between ER and vesicles/Golgi or lipid droplets. This dynamic relocalization also allows efficient and rapid cross-pathway coordination, *e.g.* between phospholipid, sterol, and sphingolipid synthesis. Future efforts will be directed toward further elucidation of this working hypothesis.

Acknowledgments—We thank Elizabeth Brazeau and Cornelia Köck for technical assistance and Martin Funk for providing plasmids. Information provided by the Bioknowledge® Library was used for the present study.

* This work was supported by grants from the Austrian Science Fund, FWF (Project F706) and the Austrian Ministry for Science, Education and Culture (Project Genomics of Lipid-associated Disorders–GOLD-C7 in the framework of the Austrian Genomics Program, GEN-AU) (to S. D. K.) and National Institutes of Health Grant P41 RR11823 (to S. F.). The costs of publication of this article were defrayed in part by the payment of page charges. This article must therefore be hereby marked "*advertisement*" in accordance with 18 U.S.C. Section 1734 solely to indicate this fact.

S The on-line version of this manuscript (available at http://www.mcponline.org) contains supplemental material.

¶ Present address: Albany Molecular Research, Inc., Bothell Research Center, 18804 North Creek Parkway, Bothell, WA 98011.

** An investigator of the Howard Hughes Medical Institute.

‡‡ To whom correspondence should be addressed. Tel.: 43-316-380-5487; Fax: 43-316-380-9857; E-mail: sepp.kohlwein@uni-graz.at.

REFERENCES

1. Tuller, G., Nemec, T., Hrastnik, C. & Daum, G. (1999) Lipid composition of subcellular membranes of an FY1679-derived haploid yeast wild-type strain grown on different carbon sources. *Yeast* **15,** 1555–1564
2. Brugger, B., Erben, G., Sandhoff, R., Wieland, F. T. & Lehmann, W. D. (1997) Quantitative analysis of biological membrane lipids at the low picomole level by nano-electrospray ionization tandem mass spectrometry. *Proc. Natl. Acad. Sci. U. S. A.* **94,** 2339–2344
3. Schneiter, R., Brugger, B., Sandhoff, R., Zellnig, G., Leber, A., Lampl, M., Athenstaedt, K., Hrastnik, C., Eder, S., Daum, G., Paltauf, F., Wieland, F. T. & Kohlwein, S. D. (1999) Electrospray ionization tandem mass spectrometry (ESI-MS/MS) analysis of the lipid molecular species composition of yeast subcellular membranes reveals acyl chain-based sorting/remodeling of distinct molecular species en route to the plasma membrane. *J. Cell Biol.* **146,** 741–754
4. Achleitner, G., Gaigg, B., Krasser, A., Kainersdorfer, E., Kohlwein, S. D., Perktold, A., Zellnig, G. & Daum, G. (1999) Association between the endoplasmic reticulum and mitochondria of yeast facilitates interorganelle transport of phospholipids through membrane contact. *Eur. J. Biochem.* **264,** 545–553
5. Pichler, H., Gaigg, B., Hrastnik, C., Achleitner, G., Kohlwein, S. D., Zellnig, G., Perktold, A. & Daum, G. (2001) A subfraction of the yeast endoplasmic reticulum associates with the plasma membrane and has a high capacity to synthesize lipids. *Eur. J. Biochem.* **268,** 2351–2361
6. Wagner, S. & Paltauf, F. (1994) Generation of glycerophospholipid molecular species in the yeast *Saccharomyces cerevisiae*. Fatty acid pattern of phospholipid classes and selective acyl turnover at sn-1 and sn-2 positions. *Yeast* **10,** 1429–1437
7. Kumar, A., Agarwal, S., Heyman, J. A., Matson, S., Heidtman, M., Piccirillo, S., Umansky, L., Drawid, A., Jansen, R., Liu, Y., Cheung, K. H., Miller, P., Gerstein, M., Roeder, G. S. & Snyder, M. (2002) Subcellular localization of the yeast proteome. *Genes Dev.* **16,** 707–719
8. Tatchell, K. & Robinson, L. C. (2002) Use of green fluorescent protein in living yeast cells. *Methods Enzymol.* **351,** 661–683
9. Kohlwein, S. D. (2000) The beauty of the yeast: live cell microscopy at the limits of optical resolution. *Microsc. Res. Tech.* **51,** 511–529
10. Huh, W. K., Falvo, J. V., Gerke, L. C., Carroll, A. S., Howson, R. W., Weissman, J. S. & O'Shea, E. K. (2003) Global analysis of protein localization in budding yeast. *Nature* **425,** 686–691
11. Hazbun, T. R., Malmstrom, L., Anderson, S., Graczyk, B. J., Fox, B., Riffle, M., Sundin, B. A., Aranda, J. D., McDonald, W. H., Chiu, C. H., Snydsman, B. E., Bradley, P., Muller, E. G., Fields, S., Baker, D., Yates, J. R., III & Davis, T. N. (2003). Assigning function to yeast proteins by integration of technologies. *Mol. Cell* 12, 1353–1365
12. Zhu, H., Klemic, J. F., Chang, S., Bertone, P., Casamayor, A., Klemic, K. G., Smith, D., Gerstein, M., Reed, M. A. & Snyder, M. (2000) Analysis of yeast protein kinases using protein chips. *Nat. Genet.* **26,** 283–289
13. Hudson, J. R., Jr., Dawson, E. P., Rushing, K. L., Jackson, C. H., Lockshon, D., Conover, D., Lanciault, C., Harris, J. R., Simmons, S. J., Rothstein, R. & Fields, S. (1997) The complete set of predicted genes from *Saccharomyces cerevisiae* in a readily usable form. *Genome Res.* **7,** 1169–1173
14. Ma, H., Kunes, S., Schatz, P. J. & Botstein, D. (1987) Plasmid construction by homologous recombination in yeast. *Gene* (*Amst*.) **58,** 201–216
15. Uetz, P., Giot, L., Cagney, G., Mansfield, T. A., Judson, R. S., Knight, J. R., Lockshon, D., Narayan, V., Srinivasan, M., Pochart, P., Qureshi-Emili, A., Li, Y., Godwin, B., Conover, D., Kalbfleisch, T., Vijayadamodar, G., Yang, M., Johnston, M., Fields, S. & Rothberg, J. M. (2000) A comprehensive analysis of protein-protein interactions in *Saccharomyces cerevisiae*. *Nature* **403,** 623–627
16. Kals, M., Natter, K., Thallinger, G. G., Trajanoski, Z. & Kohlwein, S. D. (2005) YPL.db2: the Yeast Protein Localization database, version 2.0. *Yeast* **22,** 213–218
17. Habeler, G., Natter, K., Thallinger, G. G., Crawford, M. E., Kohlwein, S. D. & Trajanoski, Z. (2002) YPL.db: the Yeast Protein Localization database. *Nucleic Acids Res.* **30,** 80–83
18. Christie, K. R., Weng, S., Balakrishnan, R., Costanzo, M. C., Dolinski, K., Dwight, S. S., Engel, S. R., Feierbach, B., Fisk, D. G., Hirschman, J. E., Hong, E. L., Issel-Tarver, L., Nash, R., Sethuraman, A., Starr, B., Theesfeld, C. L., Andrada, R., Binkley, G., Dong, Q., Lane, C., Schroeder, M., Botstein, D. & Cherry, J. M. (2004) Saccharomyces Genome Database (SGD) provides tools to identify and analyze sequences from *Saccharomyces cerevisiae* and related sequences from other organisms. Nucleic Acids Res. **32,** D311–D314
19. Mumberg, D., Muller, R. & Funk, M. (1995) Yeast vectors for the controlled expression of heterologous proteins in different genetic backgrounds. *Gene* (*Amst*.) **156,** 119–122
20. Ito, H., Fukuda, Y., Murata, K. & Kimura, A. (1983) Transformation of intact yeast cells treated with alkali cations. *J. Bacteriol.* **153,** 163–168
21. Horvath, A. & Riezman, H. (1994) Rapid protein extraction from *Saccharomyces cerevisiae. Yeast* **10,** 1305–1310
22. Mewes, H. W., Amid, C., Arnold, R., Frishman, D., Guldener, U., Mannhaupt, G., Munsterkotter, M., Pagel, P., Strack, N., Stumpflen, V., Warfsmann, J. & Ruepp, A. (2004). MIPS: analysis and annotation of proteins from whole genomes. *Nucleic Acids Res.* **32,** D41–D44
23. Cagney, G., Uetz, P. & Fields, S. (2000) High-throughput screening for protein-protein interactions using two-hybrid assay. *Methods Enzymol.* **328,** 3–14
24. Caro, L. H., Tettelin, H., Vossen, J. H., Ram, A. F., van den Ende, H. & Klis, F. M. (1997) *In silico* identification of glycosyl-phosphatidylinositol-anchored plasma-membrane and cell wall proteins of *Saccharomyces cerevisiae. Yeast* **13,** 1477–1489

25. Simpson, J. C., Wellenreuther, R., Poustka, A., Pepperkok, R. & Wiemann, S. (2000) Systematic subcellular localization of novel proteins identified by large-scale cDNA sequencing. *EMBO Rep.* **1,** 287–292
26. Ashburner, M., Ball, C. A., Blake, J. A., Botstein, D., Butler, H., Cherry, J. M., Davis, A. P., Dolinski, K., Dwight, S. S., Eppig, J. T., Harris, M. A., Hill, D. P., Issel-Tarver, L., Kasarskis, A., Lewis, S., Matese, J. C., Richardson, J. E., Ringwald, M., Rubin, G. M. & Sherlock, G. (2000) Gene ontology: tool for the unification of biology. The Gene Ontology Consortium. *Nat. Genet.* **25,** 25–29
27. Swedlow, J. R., Goldberg, I., Brauner, E. & Sorger, P. K. (2003) Informatics and quantitative analysis in biological imaging. *Science* **300,** 100–102
28. Hampton, R. Y. (2002) Proteolysis and sterol regulation. *Annu. Rev. Cell Dev. Biol.* **18,** 345–378
29. Milla, P., Athenstaedt, K., Viola, F., Oliaro-Bosso, S., Kohlwein, S. D., Daum, G. & Balliano, G. (2002) Yeast oxidosqualene cyclase (Erg7p) is a major component of lipid particles. *J. Biol. Chem.* **277,** 2406–2412
30. Leber, R., Landl, K., Zinser, E., Ahorn, H., Spok, A., Kohlwein, S. D., Turnowsky, F. & Daum, G. (1998) Dual localization of squalene epoxidase, Erg1p, in yeast reflects a relationship between the endoplasmic reticulum and lipid particles. *Mol. Biol. Cell* **9,** 375–386
31. Athenstaedt, K., Zweytick, D., Jandrositz, A., Kohlwein, S. D. & Daum, G. (1999) Identification and characterization of major lipid particle proteins of the yeast *Saccharomyces cerevisiae*. *J. Bacteriol.* **181,** 6441–6448
32. Mo, C., Milla, P., Athenstaedt, K., Ott, R., Balliano, G., Daum, G. & Bard, M. (2003) In yeast sterol biosynthesis the 3-keto reductase protein (Erg27p) is required for oxidosqualene cyclase (Erg7p) activity. *Biochim. Biophys. Acta* **1633,** 68–74
33. Prein, B., Natter, K. & Kohlwein, S. D. (2000) A novel strategy for constructing N-terminal chromosomal fusions to green fluorescent protein in the yeast *Saccharomyces cerevisiae*. *FEBS Lett.* **485,** 29–34
34. Leber, R., Zinser, E., Zellnig, G., Paltauf, F. & Daum, G. (1994) Characterization of lipid particles of the yeast, *Saccharomyces cerevisiae*. *Yeast* **10,** 1421–1428
35. Han, G., Gable, K., Kohlwein, S. D., Beaudoin, F., Napier, J. A. & Dunn, T. M. (2002) The *Saccharomyces cerevisiae* YBR159w gene encodes the 3-ketoreductase of the microsomal fatty acid elongase. *J. Biol. Chem.* **277,** 35440–35449
36. Kohlwein, S. D., Eder, S., Oh, C. S., Martin, C. E., Gable, K., Bacikova, D. & Dunn, T. (2001) Tsc13p is required for fatty acid elongation and localizes to a novel structure at the nuclear-vacuolar interface in *Saccharomyces cerevisiae*. *Mol. Cell. Biol.* **21,** 109–125
37. Pan, X., Roberts, P., Chen, Y., Kvam, E., Shulga, N., Huang, K., Lemmon, S. & Goldfarb, D. S. (2000) Nucleus-vacuole junctions in *Saccharomyces cerevisiae* are formed through the direct interaction of Vac8p with Nvj1p. *Mol. Biol. Cell* **11,** 2445–2457
38. Wright, R., Basson, M., D'Ari, L. & Rine, J. (1988) Increased amounts of HMG-CoA reductase induce "karmellae": a proliferation of stacked membrane pairs surrounding the yeast nucleus. *J. Cell Biol.* **107,** 101–114
39. Gable, K., Slife, H., Bacikova, D., Monaghan, E. & Dunn, T. M. (2000) Tsc3p is an 80-amino acid protein associated with serine palmitoyltransferase and required for optimal enzyme activity. *J. Biol. Chem.* **275,** 7597–7603
40. Cliften, P., Wang, Y., Mochizuki, D., Miyakawa, T., Wangspa, R., Hughes, J. & Takemoto, J. Y. (1996). SYR2, a gene necessary for syringomycin growth inhibition of *Saccharomyces cerevisiae*. *Microbiology* **142,** 477–484
41. Guillas, I., Kirchman, P. A., Chuard, R., Pfefferli, M., Jiang, J. C., Jazwinski, S. M. & Conzelmann, A. (2001) C26-CoA-dependent ceramide synthesis of *Saccharomyces cerevisiae* is operated by Lag1p and Lac1p. *EMBO J.* **20,** 2655–2665
42. Barz, W. P. & Walter, P. (1999) Two endoplasmic reticulum (ER) membrane proteins that facilitate ER-to-Golgi transport of glycosylphosphatidylinositol-anchored proteins. *Mol. Biol. Cell* **10,** 1043–1059
43. Eisenkolb, M., Zenzmaier, C., Leitner, E. & Schneiter, R. (2002) A specific structural requirement for ergosterol in long-chain fatty acid synthesis mutants important for maintaining raft domains in yeast. *Mol. Biol. Cell* **13,** 4414–4428
44. Simons, K. & Ikonen, E. (1997) Functional rafts in cell membranes. *Nature* **387,** 569–572
45. Thukral, S. K., Eisen, A. & Young, E. T. (1991) Two monomers of yeast transcription factor ADR1 bind a palindromic sequence symmetrically to activate ADH2 expression. *Mol. Cell. Biol.* **11,** 1566–1577
46. Murphy, D. J. & Vance, J. (1999) Mechanisms of lipid-body formation. *Trends Biochem. Sci.* **24,** 109–115
47. Sorger, D., Athenstaedt, K., Hrastnik, C. & Daum, G. (2004). A yeast strain lacking lipid particles bears a defect in ergosterol formation. *J. Biol. Chem.* **279,** 31190–31196
48. Roberts, P., Moshitch-Moshkovitz, S., Kvam, E., O'Toole, E., Winey, M. & Goldfarb, D. S. (2003) Piecemeal microautophagy of nucleus in *Saccharomyces cerevisiae*. *Mol. Biol. Cell* **14,** 129–141
49. Mo, C., Valachovic, M., Randall, S. K., Nickels, J. T. & Bard, M. (2002) Protein-protein interactions among C-4 demethylation enzymes involved in yeast sterol biosynthesis. *Proc. Natl. Acad. Sci. U. S. A.* **99,** 9739–9744
50. Brown, M. S. & Goldstein, J. L. (1997) The SREBP pathway: regulation of cholesterol metabolism by proteolysis of a membrane-bound transcription factor. *Cell* **89,** 331–340
51. Chellappa, R., Kandasamy, P., Oh, C. S., Jiang, Y., Vemula, M. & Martin, C. E. (2001) The membrane proteins, Spt23p and Mga2p, play distinct roles in the activation of *Saccharomyces cerevisiae* OLE1 gene expression. Fatty acid-mediated regulation of Mga2p activity is independent of its proteolytic processing into a soluble transcription activator. *J. Biol. Chem.* **276,** 43548–43556
52. Hoppe, T., Matuschewski, K., Rape, M., Schlenker, S., Ulrich, H. D. & Jentsch, S. (2000) Activation of a membrane-bound transcription factor by regulated ubiquitin/proteasome-dependent processing. *Cell* **102,** 577–586
53. Rape, M., Hoppe, T., Gorr, I., Kalocay, M., Richly, H. & Jentsch, S. (2001) Mobilization of processed, membrane-tethered SPT23 transcription factor by CDC48(UFD1/NPL4), a ubiquitin-selective chaperone. *Cell* **107,** 667–677
54. Stewart, L. C. & Yaffe, M. P. (1991) A role for unsaturated fatty acids in mitochondrial movement and inheritance. *J. Cell Biol.* **115,** 1249–1257
55. Tatzer, V., Zellnig, G., Kohlwein, S. D. & Schneiter, R. (2002) Lipid-dependent subcellular relocalization of the acyl chain desaturase in yeast. *Mol. Biol. Cell* **13,** 4429–4442